

See discussions, stats, and author profiles for this publication at: <https://www.researchgate.net/publication/232608137>

Theoretical study of the gas phase $\text{Sc} + (\text{NO}, \text{O}_2) \rightarrow \text{ScO} + (\text{N}, \text{O})$ reactions

ARTICLE in THE JOURNAL OF PHYSICAL CHEMISTRY A · OCTOBER 2002

Impact Factor: 2.69 · DOI: 10.1021/jp021915y

CITATIONS

5

READS

44

5 AUTHORS, INCLUDING:



Kyung Chun Kim

Pusan National University

253 PUBLICATIONS 1,625 CITATIONS

SEE PROFILE



Yoon Sup Lee

Korea Advanced Institute of Science and Tec...

211 PUBLICATIONS 4,397 CITATIONS

SEE PROFILE



Dongwook Kim

Kyonggi University

47 PUBLICATIONS 1,840 CITATIONS

SEE PROFILE

Theoretical Study of the Gas Phase $\text{Sc} + (\text{NO}, \text{O}_2) \rightarrow \text{ScO} + (\text{N}, \text{O})$ Reactions

Kyounghoon Kim and Yoon Sup Lee*

Department of Chemistry and School of Molecular Science (BK21), Korea Advanced Institute of Science and Technology, Daejeon 305-701, Korea

Dongwook Kim and Kwang S. Kim

National Creative Research Center for Supercritical Materials and Department of Chemistry, Pohang University of Science and Technology, Pohang 790-784, Korea

Gwang-Hi Jeung*

Laboratoire de Chimie Théorique (CNRS UMR6517), Case 521, Campus de St-Jérôme, Université de Provence, 13397 Marseille Cedex 20, France

Received: August 20, 2002

The potential energy surfaces concerning a moderately exoergic reaction, $\text{Sc} + \text{NO} \rightarrow \text{ScO} + \text{N}$, and a largely exoergic reaction, $\text{Sc} + \text{O}_2 \rightarrow \text{ScO} + \text{O}$, were calculated with all-electron multiconfiguration self-consistent-field and configuration interaction methods. There are activation barriers in the initial collision phase of both reactions. The end-on attack appears to be the most efficient for the first reaction, whereas the side-on attack is the most efficient for the second reaction. Two stable forms of the intermediate complex were found for the first reaction, NScO and Sc[NO] , in agreement with a recent density functional study. Similarly, two stable isomers are found for the second reaction, OScO (oxo) and $\text{Sc[O}_2]$ (peroxo), the former being more stable than the latter. We describe here the general shape of the potential energy surfaces involving these intermediates. The electron transfer from the metal atom occurs at short intermolecular distances in these reactions.

I. Introduction

The oxidation reactions of transition metals show a lot of interesting aspects that are useful in pure and applied sciences. Understanding the basic oxidation mechanism is crucial to many areas of study, such as surface science, metallurgy, aeronautical engineering, and space science. Previous experimental studies employed molecular-beam techniques combined with the spectroscopic analysis of the product^{1–3} and gas-flow measurements of the reaction rate by depletion of the atomic populations.^{4–6} A recent series of matrix-isolated infrared spectroscopic determinations on mixtures of the metal vapor and oxygen molecules has revealed different species of oxides and their vibrational frequencies were measured.⁷ Nitric oxide is also a good oxidant that produces various species of metal oxides.⁸ To better understand the oxidation reaction, it would be crucial to know what role is played by these complexes which could be produced not only as final products but also as reaction intermediates.

The ab initio calculations for the oxidation reaction involving the transition metal atoms are rather scarce, partly because of the technical difficulty originating from treatment of the *d* atomic orbitals. It is well-known that the high-level calculations are required even for diatomic molecules of transition metals to account for the electron correlation effect that varies a lot from state to state. Furthermore, a large region of the potential energy surfaces should be explored to consider not only the reactants and the products but also all possible intermediates or transition

states which might be involved in the reaction. Recently, several density functional theory (DFT) calculations have been reported for nitrosyl⁹ and oxo complexes.^{7,9–12} They often gave two stable forms, one with an obtuse O–M–O or N–M–O angle and the other with an acute angle.

Oxidation reactions of scandium studied in the gas phase by medium resolution optical techniques led to partial results about the formation of ScO in various electronic states.^{1,2} However, these results could not be fully interpreted in the absence of data over potential energy surfaces. Very recently, Luc and Vetter at Orsay have carried out an effusive-beam/diverging-flow collision experiment on the first title reaction, $\text{Sc} + \text{NO} \rightarrow \text{ScO} + \text{N}$ (1), detecting the product by continuous wave laser-induced fluorescence.¹⁴ This reaction is moderately exoergic, so that a small number of vibrational states of the ground electronic state of ScO can be populated. They have detected rotational distribution of the $X\ ^2\Sigma^+$ ($v'' = 0$) state of ScO , through the $A\ ^2\Pi$ ($v' = 1$) – $X\ ^2\Sigma^+$ ($v'' = 0$) absorption band followed by the $A(v' = 1) - X(v'' = 1)$ fluorescence.

The cross sections for the title reactions have been predicted as being very small because a high activation barrier coming from the ionic-neutral crossing has been presumed.⁴ An electron transfer from the metal atom to the oxygen atom should take place in forming a ScO molecule. The question of the electron transfer from the metal atom to the NO or O_2 moiety is an important aspect of the title reactions.

Recently, we have presented a brief account of our theoretical work together with the experiments by Vetter's group¹⁵ on the $\text{Sc} + \text{NO} \rightarrow \text{ScO} + \text{N}$ reaction (1). Another related oxidation

* To whom correspondence should be addressed. Phone: +82-42-869-2821. Fax: +82-42-869-2810. E-mail: yslee@mail.kaist.ac.kr.

reaction, $\text{Sc} + \text{O}_2 \rightarrow \text{ScO} + \text{O}$ (2), is also studied in this work. The O_2 reaction is much more exoergic than the NO reaction, and more vibrational states of ScO can be produced in the O_2 reaction. In this paper, theoretical results for the two reactions are compared with each other and also with the available experimental data.

II. Method of Computation

The molecular systems ScNO and ScO₂ including the reactants ($\text{Sc} + \text{NO}$, $\text{Sc} + \text{O}_2$), the products ($\text{ScO} + \text{N}$, $\text{ScO} + \text{O}$) and the intermediate complexes (ScNO , ScO_2) were calculated using all-electron complete active space (CAS) self-consistent-field (SCF) and the configuration interaction (CI) methods. First, we have optimized a basis set for Sc consisting of 16s11p7d Gaussian type orbitals (GTOs) to get the lowest energy of the ground state ($3d^14s^2$, 2D). The total energy calculated on the SCF level is $-759.727\,04$ hartree which is close to the Hartree–Fock (HF) limit value, $-759.735\,52$.¹⁶ The innermost GTOs were contracted to 12s9p5d atomic basis functions (ABFs), which increased the energy slightly to $-759.725\,93$. For the molecular calculations we have added 2f GTO–ABF to the Sc atom. For nitrogen and oxygen atoms, we have used the same basis set as in the TiNO and TiO₂ cases:¹⁷ 12s7p3d GTOs contracted to 8s5p3d ABFs and 3d GTO–ABF for the N and O atoms. Exponents and contraction coefficients of the present basis sets are available from the authors upon request. For the active space of CASSCF, all possible molecular orbitals initially made from 4s and 3d atomic orbitals of the scandium and 2p atomic orbitals of nitrogen and oxygen atoms were included. The number of configuration state functions (CSFs) generated in CASSCF was 141,760 (C_s symmetry) for ScNO and 84,982 (C_{2v} symmetry) for ScO₂. The MOLPRO¹⁸ and MOLCAS¹⁹ programs have been used in this work.

Several electronic states of ScO are known by electron spectroscopy^{20,21} and the $A\ ^2\Pi$ ($v' = 1$) – $X\ ^2\Sigma^+$ ($v'' = 0$) band showing a strong perturbation has been analyzed.²² The bond energy (D^0_0) of the ground state has been recently revised to 6.92 eV by Luc and Vetter¹⁴ that is slightly smaller than the previously known values, 6.95,²² 6.96,²¹ and 7.16 eV.²³ To test the accuracy of the ab initio calculation, we have calculated three electronic states of ScO, the X, A and A' $^2\Delta$ states, with an extensive multireference configuration interaction (MRCI) method. The three potential curves are given in Figure 1(a) where we can see a crossing between the A and A' states which causes the perturbation previously observed.²¹ In usual conditions, the A and A' states cannot be formed by the title reactions because the reactants do not have enough energy. Our calculated spectroscopic constants for the ground state are summarized in Table 1. Our bond energy for $v = 0$ (D^0_0), 6.62 eV, is somewhat smaller than the experimental value (6.92 eV)^{14,15} and calculated values by the coupled-cluster singles and doubles with perturbed triples [CCSD(T)] method (6.90 eV)²⁴ and DFT (7.76 eV).¹² It is common that the variational methods tend to underestimate the bond energy even at the very high level of theory such as MRCI compared with the CCSD(T) method while DFT usually overestimates the bond energy. Other spectroscopic constants in Table 1, R_e and ω_e , are in excellent agreement with one another. It can also be seen from Table 1 that our data is significantly closer to the experimental values than previous data obtained by using effective-core potentials.²⁵

The dipole moment of the ground state of ScO as a function of the interatomic distance is drawn in Figure 1b. There is a sudden electron transfer from the metal atom to the oxygen atom

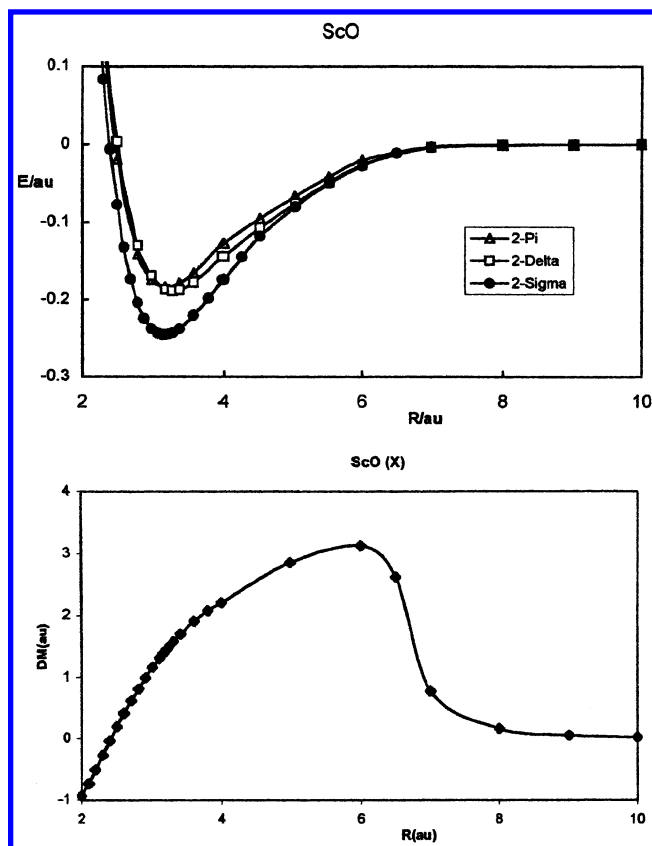


Figure 1. (a) Potential energy curves (MRCI) for the three lowest electronic states of ScO (in a.u.). (b) Dipole moment of the ground state of ScO (in a.u.).

TABLE 1: Spectroscopic Constants for the Ground Electronic States $^2\Sigma^+$ of ScO (This Work from MRCI Calculations)

	this work	expt	CCSD(T) ^a	DFT ^b	ECP ^c
R_e (pm)	169	166.8 ^d	167.9	166.5	163
ω_e (cm ⁻¹)	970	964.95 ^d	971	972	1120
D^0_0 (eV)	6.62	6.92 ^e	6.90	7.76	5.21

^a Reference 24. ^b DFT calculations with the BPW91 functional from ref 12. ^c Effective core potential calculations from ref 25. ^d Reference 13. ^e Reference 15.

around 6–7 bohr. In this zone, there occurs a strong avoided crossing between the neutral configuration, $\text{Sc}(3d^14s^2)/\text{O}$, and the ionic configuration, $\text{Sc}^+(3d^14s^1)/\text{O}^-$. For the bond formation between Sc and O atoms in the reactions (1) and (2), the metal atom should donate an electron during the collisional phase.

The ionization potential of the Sc atom, from $\text{Sc } 3d^14s^2$ (2D) to $\text{Sc}^+ 3d^14s^1$ (3D), was calculated to be 6.33 eV which is quite close to the experimental value, 6.56 eV.²⁶ The energy balance of the reaction (1) calculated with our basis set in the CASSCF method is -0.69 eV (the negative sign signifying the exoergicity) which is quite close to the experimental value of -0.67 eV (supposing $D^0_0(\text{ScO}) = 6.92$ eV^{14,15}), probably due to a fortuitous cancellation of errors. The energy balance of the reaction (2) calculated with our basis set in the CASSCF method, -2.66 eV, is significantly lower than the experimental data, -2.00 eV.

The single-and-double configuration interaction (SDCI) has been performed for a limited number of ScNO and ScO₂ CASSCF geometries because of the great amount of computer time required for each geometry. The molecular orbitals have been taken from the above CASSCF result, but the reference space is considerably smaller than that of the CASSCF

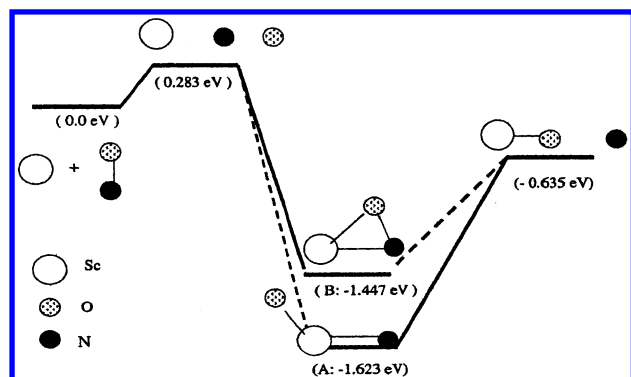


Figure 2. Potential energy (CASSCF) diagram for the $\text{Sc} + \text{NO} \rightarrow \text{ScO} + \text{N}$ reaction. All energies are without zero-point vibration energies.

calculation. All possible single and double excitations of 10 (ScNO) or 11 (ScO_2) valence electrons were included for the reference CSFs.

III. Results

Sc + NO. The initial collisional phase of the reaction (1) has been studied by checking two different geometrical approaches between Sc and NO. One is the C_s point group symmetry where the Sc atom approaches the NO group with the Sc–O and Sc–N distances kept equal, i.e., a side-on collision. The other is the collinear ($C_{\infty v}$) geometry, an end-on collision. The side-on posed a problem of convergence around the activation barrier where the ionic and neutral configurations intermix. The end-on collision had no convergence problem and the activation barrier appeared to be lower. The lowest barrier occurs for the ScNO geometry and not the ScON . It may be due to a less steric repulsion between the metal atom and the NO moiety in the former geometry than in the latter since the O atom has one σ electron pair while the N atom does not. The activation energy, calculated as the energy difference between the lowest barrier point and the energy of noninteracting reactants at infinity, is 0.17 eV (0.28 eV without zero-point-energy corrections) at the CASSCF level and 0.19 eV (0.30 eV without zero-point-energy corrections) at the SDCl level. The addition of the dynamic electron correlation effect slightly elevates the barrier as was the case in $\text{Ti} + \text{NO}$.¹⁷ After surmounting this barrier, the NO moiety rotates around the metal center to form a side-on complex and the electron transfer occurs from the metal atom to the NO molecule. Figure 2 shows the energy diagram (in CASSCF) of the $\text{Sc} + \text{NO} \rightarrow \text{ScO} + \text{N}$ reaction.

We found two intermediate complexes which can be written as NScO (with the obtuse N–Sc–O angle; A in Figure 2) and Sc[NO] (with the acute N–Sc–O angle; B in Figure 2). The complex B is connected with the reactants on a single potential surface. We have explored many different paths connecting A and B, and checked that all led to the barriers with energies higher than the reactants, confirming that both of those two forms are stable isomers. We used solid lines in Figure 2 for the cases where we have effectively obtained continuous potential energy surfaces connecting two geometries, whereas we have used broken lines for the part where we could not obtain continuous potential energy surfaces for connecting geometries. We could obtain a single potential surface connecting the isomer A and the products.

We report the relative energies for the lowest electronic states of ScNO , their geometrical parameters and the net charges of the metal atom in Table 2. The geometrical parameters

calculated in the density functional method by Kushto et al.⁸ and those calculated in this work by the all-electron ab initio method are fairly close, but the relative energies calculated in the two methods are in disorder. In particular, the singlet state ($^1A'$) appeared to be practically level with the triplet Sc[NO] state ($^3A''$) and the triplet NScO state ($^3A''$) is 0.37 eV higher than the triplet Sc[NO] state in DFT, whereas our result places two triplet states significantly lower than the singlet state. To clarify this problem, we have repeated the DFT calculation with the BP86 functional using our own basis set which is believed to be more flexible than Kushto's (14s9p5d contracted to 8s4p3d for the metal atom and 6-31+G* for N and O). Our DFT result reproduces Kushto's DFT ordering of the energy, placing the singlet state lower than the triplet state, as can be seen in Table 2, although the singlet–triplet energy difference in our calculation (0.47 eV) is larger than Kushto's (0.37 eV). On the other hand, our minimum energy geometries are somewhat different from Kushto's. In particular, the O–Sc–N bond angle calculated in our DFT, 124.2°, is closer to our CASSCF value, 126.9°, than to the Kushto's value, 112.7°. Using the molecular geometry of the DFT calculation, we have included further electron correlation effect with the coupled-cluster singles, doubles, and noniterative inclusion of triple excitations [CCSD-(T) in Table 2] calculation for the complexes. It gave the two triplets and the singlet about the same energies. Furthermore, the isomer B appeared to be more stable than the isomer A by 0.06 eV. We have carried out the SDCl calculation at the minimum energy geometries from CASSCF. It produces practically the same energy (Table 2) for the $^3A''$ state of NScO and the $^1A'$ state of Sc[NO] . The singlet state contains the dynamic correlation energy substantially larger than the triplet states. Because the present work does not treat the potential energy surface of the singlet states, CASSCF results can be reasonably trusted without considering corrections due to the dynamic correlation effect.

Concerning the charge distribution in the lowest-energy form of the complex (A), NScO , about 4/3 of the metal electron is transferred to the N and O atoms. In the Sc[NO] isomer (B), about 3/4 of the metal electron is transferred to the NO moiety. The higher ionicity between the metal atom and the ligand atoms in the NScO isomer in comparison to the Sc[NO] is in line with our stability order; the former being more stable than the latter.

Sc + O_2 . The energy level diagram for the reaction (2) is drawn in Figure 3 and the energies and geometrical parameters of the ScO_2 complex can be found in Table 3. In this case again, there is an activation barrier due to an avoided crossing between a neutral configuration, $\text{Sc}^0(\text{O}_2)^0$, and an ionic configuration, $\text{Sc}^+(\text{O}_2)^-$. The lowest activation barrier lies in a side-on geometry and the height of the activation energy was calculated to be 0.19 eV (0.31 eV without zero-point-energy corrections) at the CASSCF level and 0.20 eV (0.33 eV without zero-point-energy corrections) at the SDCl level of calculation. In the repulsive long distance region, the metal electrons in the $4s^2-3d^1$ configuration interact mainly with the π electrons of the oxygen molecule. After the barrier is passed, the electron transfer occurs from the metal atom to the oxygen molecule as can be seen in Figure 4. The metal atom is then approximately in the $4s^13d^1$ configuration.

There are two isomers of ScO_2 as in the ScNO case, which may be represented as OScO (an oxo-complex with an obtuse O–Sc–O angle; A in Figure 3) and $\text{Sc[O}_2]$ (a peroxo-complex with an acute O–Sc–O angle, B in Figure 3). The isomer A is lower in energy than the isomer B by 1.36 eV at the CASSCF level. Our geometry optimization has been performed in the C_s

TABLE 2: Minimum Energy Geometries, Harmonic Vibrational Frequencies,^a Metal Charges and the Energy Levels of the ScNO Complex (*R* in pm, \angle in degree, ω in cm^{-1} , *Q* in a.u., and ΔE in eV)

method	state	<i>R</i> (Sc–O)	<i>r</i> (Sc–N)	\angle (O–Sc–N)	ω_1	ω_2	ω_3	<i>Q</i> (Sc)	ΔE
CASSCF	¹ A'	186	182	49.5				1.04	0.765
	³ A''(B)	196	195	40.8	470	608	1093	0.74	0.176
	³ A''(A)	169	224	126.9	149	445	942	1.30	0.0
SDCI ^b	¹ A'	186	182	49.5					0.025
	³ A''(B)	196	195	40.8					0.234
	³ A''(A)	169	224	126.9					0.0
BP86 ^c	¹ A'	184	181	49.3	490	641	885		–0.368
	³ A''(B)	195	195	40.3	481	601	1091		–0.365
	³ A''(A)	170	211	112.7	152	459	914		0.0
BP86 ^d	¹ A'	183	181	49.9					–0.468
	³ A''(B)	194	194	40.5					–0.481
	³ A''(A)	170	196	124.2					0.0
CCSD(T) ^e	¹ A'	183	181	49.9					0.132
	³ A''(B)	194	194	40.5					–0.057
	³ A''(A)	170	196	124.2					0.0
exp ^c	³ A''(B)					644	866		
	³ A''(A)					471	910		

^a ω_1 refers to a harmonic vibrational frequency for the calculation or a fundamental frequency for the experiment. ^b SDCI at the geometries of CASSCF. ^c Reference 8. ^d BP86 using our basis sets. ^e CCSD(T) at the geometries of *d*.

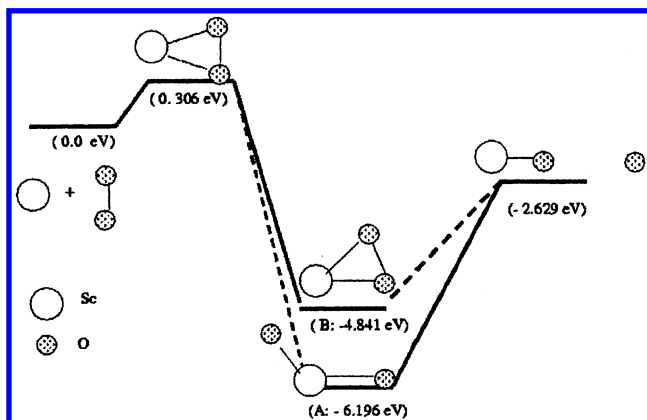


Figure 3. Potential energy (CASSCF) diagram for the $\text{Sc} + \text{O}_2 \rightarrow \text{ScO} + \text{O}$ reaction. All energies are without zero-point vibration energies.

TABLE 3: CASSCF Calculated Minimum Energy Geometries, Metal Charges and the Energy Levels of the ²A' State of ScO₂ Complex (*R* in pm, \angle in degree, *Q* in a.u., and ΔE in eV)

isomer	reference	<i>R</i> (Sc–O)	<i>R</i> (Sc–O')	\angle (O'–Sc–O)	<i>Q</i> (Sc)	ΔE
Sc[O ₂](B)	this work	187	187	48.8	0.86	1.36
	12	186	186	47.3		1.57
	7	187	187	47.1		1.43
OScO(A)	this work	170	205	125.4	1.40	0.0
	12	177	177	129.2		0.0
	7	178	178	125.9		0.0

symmetry, and yielded asymmetric Sc–O distances, 170 pm (Sc–O) and 205 pm (Sc–O'). Previous DFT calculations^{7,9} reported *C*_{2v} geometries for the two isomers. We do not know whether their optimizations were in *C*_s or *C*_{2v} symmetry. Matrix-isolated infrared spectroscopy⁷ has demonstrated the existence of the OScO isomer with the O–Sc–O bond angle of 128°. Our calculated value, 125°, as well as the DFT values, 126°⁷ and 129°¹² are close to this experimental value. Because the energy difference between the two isomers were calculated to be significantly large in the DFT calculations as well as in ours, we do not think that further electron correlation effect will change the order of stability.

A gas-phase mass spectrometry of the ScO₂ complex²⁷ estimated the bond energy of the second oxygen atom to ScO, i.e., the endoergicity of the reaction $\text{OScO} \rightarrow \text{ScO} + \text{O}$, to be 3.95 eV. Our calculated OSc–O bond energy without taking

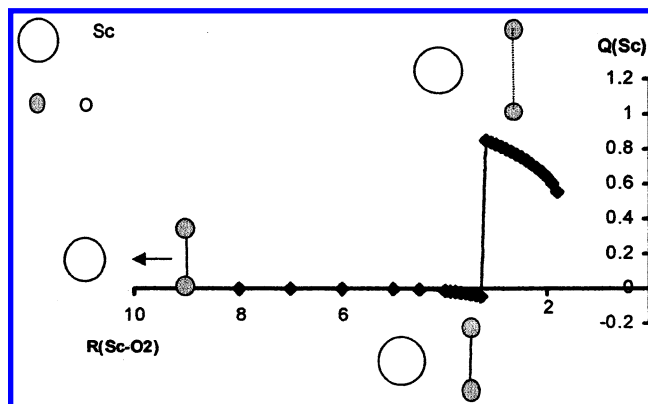


Figure 4. Net charge of the metal atom in the $\text{Sc} + \text{O}_2 \rightarrow \text{ScO} + \text{O}$ reaction (*R* in Å and *Q* in a.u.).

the zero point energies into account (Figure 3) is 3.57 eV at the CASSCF level. The DFT calculation using the BPW91 functional by Gutsev et al.⁹ estimated this bond energy to be 4.5 eV. No stable superoxo complex, which may be written as ScOO (end-on species), has been found in our calculation and no experimental observation for the superoxo complex has been reported until now. The exoergicity of this reaction, (2), is much larger than that of the $\text{Sc} + \text{NO}$ case, (1), and the ScO₂ intermediates are more strongly bonded than the ScNO.

IV. Discussion

In Luc and Vetter's experiment, the activation energy of the $\text{Sc} + \text{NO}$ reaction has been estimated to be lower than 0.10 eV,^{14,15} which is much smaller than our ab initio value, 0.17 eV (CASSCF) or 0.19 eV (SDCI). The same is expected to be the case for the activation energy of the $\text{Sc} + \text{O}_2$ reaction. Our calculated activation energy for Sc–NO is about the same as that of the Ti–NO system, 0.18 eV (CASSCF) or 0.23 eV (SDCI).¹⁷ However, the activation energy differs substantially for dioxygen cases: 0.19 eV (CASSCF) or 0.20 eV (SDCI) for the Sc–O₂ vs 0.37 eV (CASSCF) or 0.42 eV (SDCI) for the Ti–O₂.¹⁷ The electron correlation effect slightly elevates the activation barrier as we saw in the $\text{Sc} + \text{NO}$, Ti + NO (from 0.18 to 0.23 eV) and Ti + O₂ (from 0.47 to 0.52 eV)¹⁷ cases. For the reactions with dioxygen, the initial attack occurs preferentially through a side-on geometry in contrast to the nitric oxide case. The oxygen molecule has a nonbonding σ electron

pair while the nitrogen atom in the nitrogen monoxide has an unpaired π radical electron. So the end-on approach for the oxygen molecule is expected to lead to a larger repulsion, whereas the end-on approach for the nitrogen monoxide by the nitrogen side could lower the repulsion. This may explain why an end-on collision is lower in energy in the Sc–NO case and a side-on collision is lower in energy in the Sc–O₂ case. In the end-on collision, the unpaired π radical electron of the nitrogen monoxide molecule does not come into direct contact with the metal valence electron, which may be fundamental in explaining the small difference in the activation barrier between the two systems.

Using the conservation of the angular momentum before and after the collision, we could estimate the reactive cross section for the Sc + NO reaction and the impact parameter corresponding to this cross section. Our value of 2.9 Å² is in quite good agreement with the experimentally deduced value, 3.2 Å².¹⁵

In the work of Luc and Vetter on Sc + NO,^{14,15} the profile of the absorption bands was analyzed to measure the rotational distribution of the ScO product. It could not be interpreted by a pure prior statistical distribution but rather by a weak “surprisal” with $f_r = 0.6$, which means that the lifetime of the intermediate is relatively long, but not long enough to erase the memory of the rotational excitation provided by the initial angular momentum transferred by the collision. The lifetime of the intermediate complex should play a crucial role. As the initial reactant energy level is much higher than the two isomer energies and the intermediates are much more stable than both the reactants and the products, higher energy levels, both electronically and vibrationally, of the isomers can be populated in the early stage. It can then evolve to the lower level of the two isomers and also to the low vibrational levels ($v'' = 0,1$) of the product ScO. It is also important to know the branching ratios for these three possible reaction paths leading to each of NScO, Sc[NO], and ScO (or OScO, Sc[O₂] and ScO) to understand the complete reaction mechanism, which is beyond the scope of the present work.

Our work is in agreement with the reaction mechanism proposed by Kushto et al.⁸ We have confirmed that the Sc[NO] can be directly produced from Sc + NO because we found a path connecting them on the single potential energy surface. However, this reaction involves a large excess energy so that the Sc[NO] complex may undergo a rovibrational relaxations. No further reaction may be possible from this point as we did not find an energetically allowed path connecting Sc[NO] and NScO. Kushto et al.⁸ reported a photolysis of the N–O bond in Sc[NO] followed by a formation of the NScO isomer through insertion, implying a large energy barrier on the path to convert one isomer to the other. On the other hand, as the NScO isomer is connected to the product channel, it is reasonable to assume several possible reaction paths. The first step may be the reaction $\text{Sc} + \text{NO} \rightarrow (\text{NScO})^*$ where the excitation could be only rovibrational or also electronic. We cannot affirm this since we did not attempt to connect electronically excited states of the NScO isomer to the reactants. Then three possibilities can be envisaged. One possibility is the rovibrational or electronic relaxation of the complex to the ground state of NScO. Another is $(\text{NScO})^* \rightarrow \text{ScO} + \text{N}$ and the remaining possibility is $(\text{NScO})^* \rightarrow \text{ScN} + \text{O}$.

The experiment for the Sc+O₂ by Liu and Parson¹ has shown that the rotational distribution of ScO is not statistical at all. The main difference of the Sc + O₂ reaction in comparison with the Sc + NO reaction is that the former is much more exoergic. The large exoergic of the Sc + O₂ reaction may

make the reaction with oxygen molecule much faster than that with nitrogen monoxide signifying less time spent in the intermediate state, thus explaining the nonstatistical distribution of the reaction product.

Although the Sc + NO reaction is much less exoergic than the Sc + O₂ reaction, the overall reaction rate of the first reaction is measured to be more efficient than the second reaction in Ritter and Weisshaar's study.⁴ Their estimated cross section for the first reaction is 1.68 Å² while that of the second reaction is 1.01 Å². Because our calculated reaction barriers are about the same in both reactions, other dynamic factors may be responsible for this difference. Concerning the spin-state of the Sc + NO reaction because the reactant state is either triplet or singlet and the product state (ground state) can be triplet or quintet, we can infer that the triplet complex states may be more relevant to the reaction than the singlet state.

Our work confirmed the existence of two stable isomers for the ScNO and ScO₂ complexes. We have also shown the essential features of the potential energy surface involved in the reaction and the likely reaction pathways. However, we have raised several unanswered questions, which will have to wait for more reliable experiments and quantum chemical calculations.

Acknowledgment. This work was partly supported by the Korea Science and Engineering Foundation (No. 2000-121-10-2), the Supercomputing Application Support Program of KISTI, and the Creative Research Initiatives of the Korean Ministry of Science and Technology. One of the authors (Y.S.L.) acknowledges the support of the Center for Nanotubes and Nanostructured Composites. We are grateful to Professor A. J. Buglass for kindly reading the manuscript.

References and Notes

- (1) Manos, D. M.; Parson, J. M. *J. Chem. Phys.* **1975**, *63*, 3575; Liu, K.; Parson, J. M. *J. Chem. Phys.* **1977**, *67*, 1814; Manos, D. M.; Parson, J. M. *J. Chem. Phys.* **1978**, *69*, 231; Parson, J. M.; Geiger, L. C.; Conway, T. J. *J. Chem. Phys.* **1981**, *74*, 5595.
- (2) Chalek, C. L.; Gole, J. L. *J. Chem. Phys.* **1976**, *65*, 2845; Dubois, L. H.; Gole, J. L. *J. Chem. Phys.* **1977**, *66*, 779.
- (3) Naulin, C.; Hedgecock, I. M.; Costes, M. *Chem. Phys. Lett.* **1997**, *266*, 335; Vetter, R.; Naulin, Ch.; Costes, M. *Phys. Chem. Chem. Phys.* **2000**, *2*, 643.
- (4) Ritter, D.; Weisshaar, J. C. *J. Phys. Chem.* **1989**, *93*, 1576; Ritter, D.; Weisshaar, J. C. *J. Phys. Chem.* **1990**, *94*, 4907.
- (5) Brown, C. E.; Mitchell, S. A.; Hackett, P. A. *J. Phys. Chem.* **1991**, *95*, 1062.
- (6) Clemmer, D. E.; Honma, K.; Koyano, I. *J. Phys. Chem.* **1993**, *97*, 11 480.
- (7) Chertihin, G. V.; Andrews, L.; Rosi, M.; Bauschlicher, C. W., Jr. *J. Phys. Chem.* **1997**, *101*, 9085; Chertihin, G. V.; Andrews, L.; Rosi, M.; Bauschlicher, C. W., Jr. **1995**, *99*, 6356.
- (8) Kushto, G. P.; Zhou, M.; Andrews, L.; Bauschlicher, C. W., Jr. *J. Phys. Chem.* **1999**, *103*, 1115.
- (9) Bauschlicher, C. W., Jr.; Langhoff, S. R.; Partridge, H.; Sodupe, M. *J. Phys. Chem.* **1993**, *97*, 856; Bauschlicher, C. W., Jr.; Zhou, M.; Andrews, L.; Johnson, J. R. T.; I. Panas Snis, A.; Roos, B. O. *J. Phys. Chem.* **1999**, *103*, 5463.
- (10) Lyne, P. D.; Mingos, D. M. P.; Ziegler, T.; Downs, A. J. *Inorg. Chem.* **1993**, *32*, 4785.
- (11) Hrušák, J.; Koch, W.; Schwarz, H. *J. Chem. Phys.* **1994**, *101*, 3989.
- (12) Gutsev, G. L.; Rao, B. K.; Jena, P. *J. Phys. Chem. A* **2000**, *104*, 11961.
- (13) Lambert, D. L. In *Molecules in the Stellar Environment*; Jorgensen, U. G., Ed.; Springer-Verlag: Berlin 1994.
- (14) Luc, P.; Vetter, R. *J. Chem. Phys.* **2001**, *115*, 11 106.
- (15) Jeung, G.-H.; Luc, P.; Vetter, R.; Kim, K. H.; Lee, Y. S. *PCCP* **2002**, *4*, 596.
- (16) Clementi, E.; Roetti, C. *Atom. Data Nucl. Data Tables* **1974**, *14*, 177.

- (17) Kim, K. H.; Lee, Y. S.; Moon, J.-H.; Kim, Y.; Jeung, G.-H., to be published.
- (18) A package of ab initio program written by Werner, H. J.; Knowles, P. J. with contributions from Almlöf, J.; Amos, R. D.; Deegan, M. J. O.; Elbert, S. T.; Hampel, C.; Meyer, W.; Peterson, K.; Pitzer, R.; Stone, A. J.; Taylor, P. R.; Lindh, R. (1996).
- (19) Version 4: Andersson, K.; Blomberg, M. R. A.; Fülcher, M. P.; Karlström, G.; Lindh, R.; Malmqvist, P.-Å.; Neogrády, P.; Olsen, J.; Roos, B. O.; Sadlej, A. J.; Schütz, M.; Seijo, L.; Serrano-Andrés, L.; Siegbahn, P. E. M.; Widmark, P.-O. Lund University 1997.
- (20) Huber, K. P.; Herzberg, G. In *Constants of Diatomic Molecules*; Van Nostrand Reinhold: New York 1979.
- (21) Rice, S. F.; Childs, W. J.; Field, R. W. *J. Mol. Spectrosc.* **1989**, 133, 22.
- (22) Rostai, M.; Wahlbeck, P. G. *J. Chem. Thermodyn.* **1999**, 31, 255.
- (23) Ames, L. L.; Walsh, P. N.; White, D. J. *Phys. Chem.* **1967**, 71, 2707.
- (24) Bauschlicher, C. W., Jr.; Maitre, P. *Theor. Chim. Acta* **1995**, 90, 189.
- (25) Jeung, G.-H.; Koutecký, J. *J. Chem. Phys.* **1988**, 88, 3747.
- (26) Moore, C. E. *Atomic Energy Levels*; NBS (US), Circular 467, 1971; Vol. 2.
- (27) Clemmer, D. E.; Dalleska, N. F.; Armentrout, P. B. *Chem. Phys. Lett.* **1992**, 190, 259.